Edelweiss Applied Science and Technology
ISSN: 2576-8484
Vol. 9, No. 4, 651-662
2025
Publisher: Learning Gate
DOI: 10.55214/25768484.v9i4.6037

Discrete element simulation analysis of ball mill ball trajectory and liner plate structure based on EDEM

Jun Shen[1,2], Wenwei Li[1,2], Weina Deng[1*], Mingrong Huang[3]
[1]College of Mechanical Engineering, Hunan Mechanical&electrical Polytechnic, Changsha 410151, Hunan, China; 106550944@qq.com (W.D.).
[2]Manufacturing and Materials Research Unit, Department of Manufacturing Engineering, Faculty of Engineering, Mahasarakham University, Mahasarakham 44150, Thailand.
[3]Hunan Yunjian Group Co., Ltd, Changsha 410137, Hunan, China.

Abstract: The ball mill is the preferred equipment for ore grinding, and research on ball mill grinding technology can save energy and reduce energy consumption. The discrete element method is a numerical approach used to simulate the behavior of granular materials and has been widely applied in the study of mineral processing and crushing processes. This article uses EDEM discrete element software to simulate three different liner structures of ball mills (stepped liner, T-shaped liner, and inclined liner) and analyzes the motion path of grinding balls in the ball mill. At the same time, by evaluating the grinding ball height, power, collision type, collision frequency, and relative velocity of the ball mill, the grinding effect of the three lining plate structures was assessed, and it was found that the stepped lining plate has certain advantages in its grinding effect. The EDEM discrete element simulation is in good agreement with the actual working conditions of the ball mill and has good reference and guidance significance for grinding work.
Keywords: *Ball mill, EDEM simulation, Grinding ball trajectory, Liner plate structure.*

1. Introduction

The ball mill is the most historical and widely used grinding equipment in the field of grinding industry Matsanga, et al. [1] with advantages such as high crushing ratio and crushing capacity, and the ability to work continuously for a long time. The annual electricity consumption of grinding equipment accounts for 2% of the world's electricity consumption [2, 3]. Therefore, studying the performance of ball mills and improving the performance and grinding efficiency of pre mills has become one of the important ways to achieve energy conservation and consumption reduction in mineral processing equipment [4, 5]. In the past, the method of combining theory with experiment is often used to study the working performance of ball mill. Theoretical analysis has some assumptions and simplifications on the conditions in the actual grinding process, which has its own limitations. In terms of experiment, due to high opening cost of ball mill and large experiment cost, experts and scholars often use small experimental machine to carry out experimental research. However, there are many factors in the grinding process and the correlation degree is large, so it is difficult to obtain accurate data. With the rapid development of science and technology, the appearance of numerical simulation methods provides new ideas for solving the grinding production problems of mill. Finite element, discrete element and other numerical simulation methods are more and more widely used in grinding production, which can well explore the energy consumption and grinding effect of ball mill in the early stage, and have certain economic benefits

History: Received: 13 January 2025; Revised: 17 March 2025; Accepted: 21 March 2025; Published: 7 April 2025
* Correspondence: 106550944@qq.com

At present, numerical simulation software based on discrete element method is widely used in the fields of crushing and grinding [6, 7]. EDEM is the representative discrete element simulation software AmanNejad and Barani [8]; ZHANG, et al. [9]. Mu, et al. [10] and Cai, et al. [11] analyzed the compression crushing and energy consumption of single particle materials in crushers and ball mills using the discrete element method. Kim et al. investigated the effects of ball to powder diameter ratio (BPDR) and powder particle shape on EDEM simulation results and time in planetary ball millsKim, et al. [12]. Li [13] used discrete element simulation to study the optimal operating parameters of vibrating screens from amplitude, frequency, which were consistent with actual experimental results[13].

This article uses the discrete element software EDEM to simulate and experimentally study the working process of ball mills. Understand the motion trajectory and working process of grinding balls under three different lining plate structures of ball mills, and analyze the evaluation indicators based on the grinding ball height, power, collision type, collision frequency, and relative velocity of different lining plate ball mills, providing a basis for optimizing the structure and improving the performance of ball mill lining plates.

2. Simulation Experiment

2.1. Principles of Discrete Element Simulation

The basic idea of the discrete element method is to regard the medium as composed of a series of discrete and independent moving elements (particles), which conforms to the essence of the particle set [14]. Given the size and physical properties of the particle unit, the motion equation of each particle is established by Newton's second law, and the new displacement of the particle is determined by using the center difference method [15]. In the simulation process, the motion characteristics (velocity, acceleration, etc.) of each particle at a specific time are calculated by the contact force, moment and unbalanced force and moment generated by the collision between adjacent particles, and the motion characteristics of the whole system are reflected by the characteristics of each particle [16]. In EDEM software, each particle in the object is considered as an independent unit, and there is contact and separation between the units. Hertz-Mindlin non-sliding contact model is adopted for element contact [17, 18].

Normal contact force formula

$$F_n = -K_n \delta^{3/2} + C_n v_n \qquad (1)$$

Where K_n is the normal stiffness; δ is the normal overlap; C_n is the normal damping coefficient; v_n is the normal relative velocity.

Tangential contact force formula

$$F_i = k_i \int \delta_\tau dt + C_t v_t \qquad (2)$$

Where k_t is the tangential stiffness; δ_τ is the tangential displacement of the contact point; C_t is the tangential damping coefficient; v_t is the tangential relative velocity.

When the tangential force calculated by Equation (2) is greater than the friction force $\mu_s F_n$, relative sliding occurs between particles, and the tangential force formula as follow.

$$F_t = \mu_s |F_n| n_t \qquad (3)$$

2.2. Grinding Process Modeling Principle

The grinding process modeling principle of EDEM discrete element software is mainly to bond the surrounding small particles at a certain time point, and the cohesive force between the small particles can be set according to the simulated material properties. As long as the external force is greater than the cohesive force, the cohesive bond will break, and the small particles will be separated from the cohesive body, so as to realize the simulation of particle crushing process (as shown in Fig. 1). The number of bond breakage can be used as the special function data of EDEM material crushing simulation, and can be used as an index to measure the damage degree of particles, which can be applied to the study on grinding effect of ball mill working parameters.

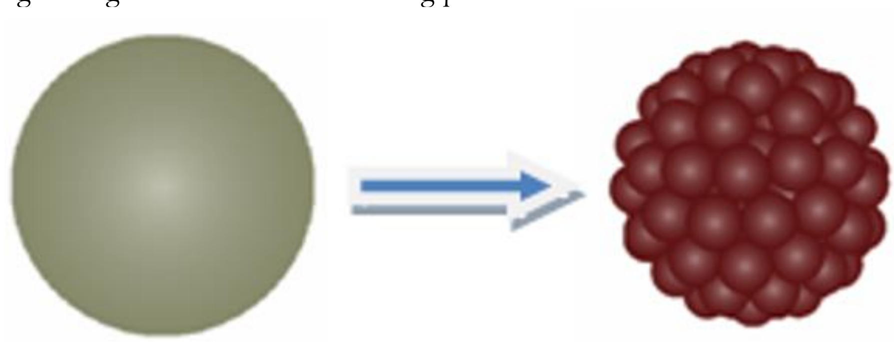

Figure 1.
The picture of particles bonding.

2.3. Establishment of Simulation Model

This experiment is based on the 5070A ball mill of a mining group in Sichuan Province, China. The most typical lining plate structures in three mines are selected for simulation (stepped liner plate, T-shaped liner plate, and Ramp liner plate). Due to the large amount of simulation data, the size of the simulation cylinder is taken as a section with a length of 120mm. The simulation time is based on reaching the equilibrium position (8s). The specific simulation parameters and discrete element parameters are set as follows.

Table 1.
Simulation parameters.

Type of liner plate	**Stepped liner plate**	**T shaped liner plate**	**Ramp liner plate**
Height of liner plate/mm	80	115	65
Barrel size of ball mill	Length of Axial length:120mm，diameter:5000mm		
Simulation run time/s	8		
Mill fill rate	24.75%		
Ratio of ball diameter	60:50:40:30=2:2:1:1		
Ball mill revolutions/rpm	14.5		
Poisson's ratio	0.3		
Coefficient of static friction	0.2		
Rolling friction coefficient	0.05		
Shear modulus /Pa	7×10^{10}		

The simulation of ball mill with three different structure liners is shown in Figure 1.

DOI: 10.55214/25768484.v9i4.6037

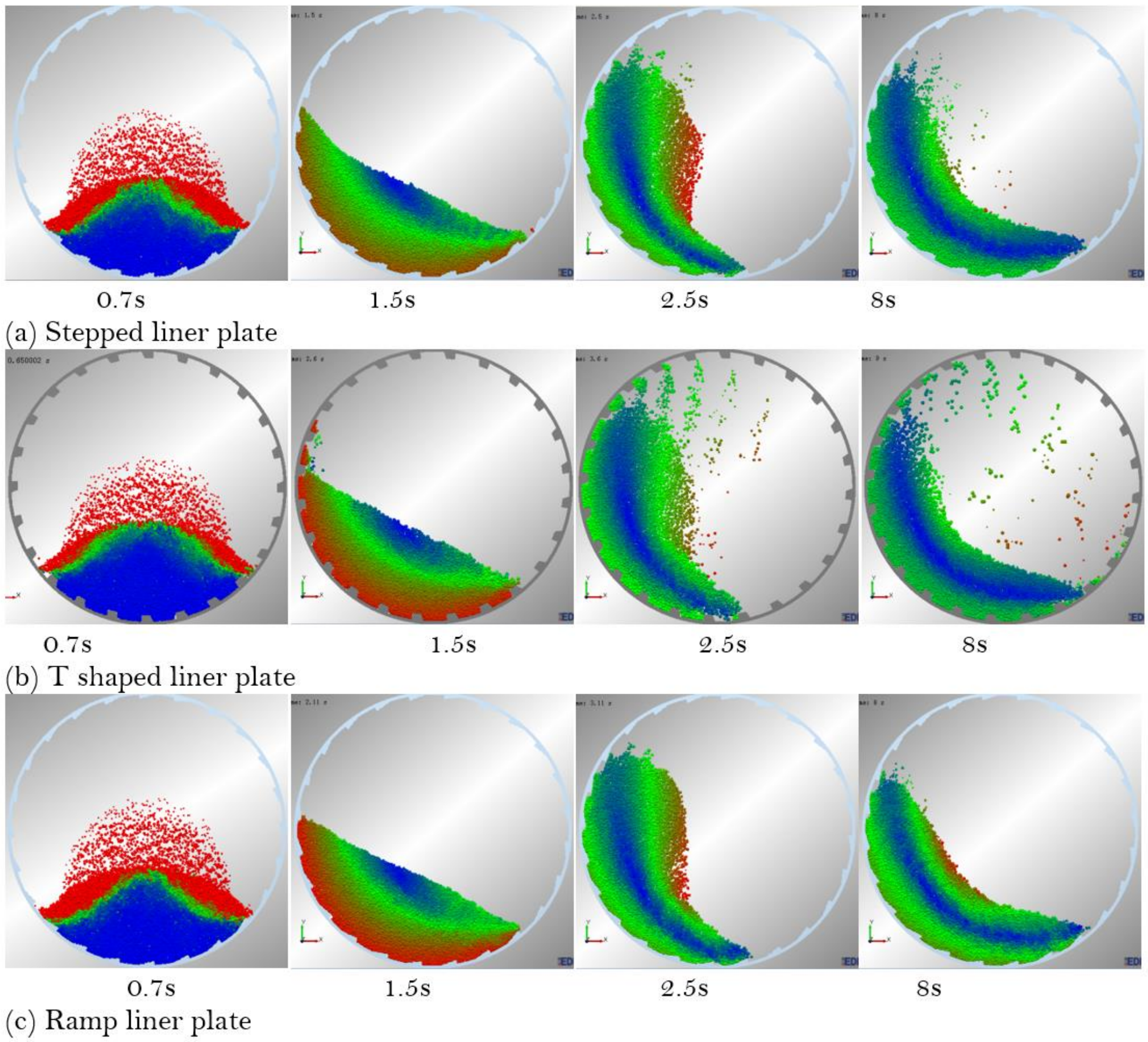

Figure 2.
Simulation of Grinding Process of Ball Mill under Different Lining Structure.

The color of the grinding ball represents speed, with red indicating the highest speed and blue indicating the lowest speed [19]. From Figure 2, it can be seen that during the generation stage of grinding ball particles to the first lifting stage at 1.5 seconds, due to the relatively small relative motion between the grinding media, the difference in their states is not significant; However, starting from 2.5 seconds, due to differences in the structure of the lifting strip of the lining plate, the movement and distribution of the grinding ball after being lifted have shown significant differences. In the ball mill with stepped liner, the ball is mainly cataract motion, with a small amount of throwing motion. The right part of the T shaped liner plate has a noticeable throwing motion, while the ramp liner plate is mainly in a downward manner.

DOI: 10.55214/25768484.v9i4.6037

3. Results and Discussion

3.1. Analysis of Grinding Ball Trajectory

EDEM is a discrete element software, whose core is that each unit cell is a discrete individual [20]. The author randomly selects a single different grinding ball near the cylinder and the outermost layer for tracking analysis, and depicts the motion trajectory inside the ball mill (Figure 2).

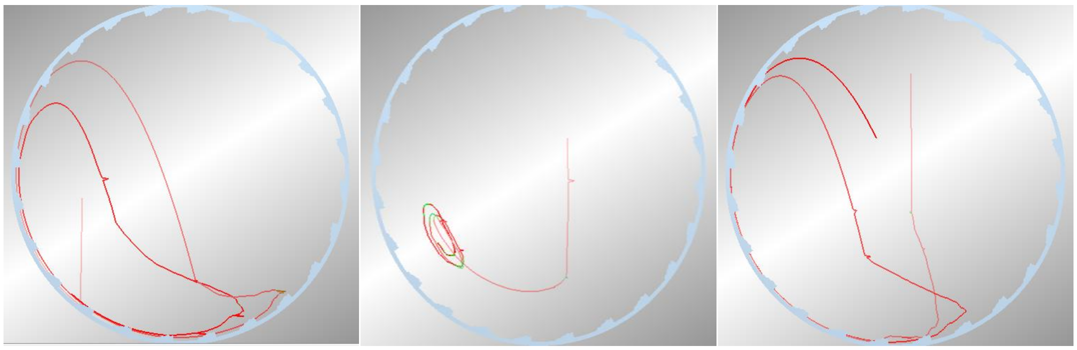

(a)Close to the cylinder ball (b) Intermediate dead zone ball (c) Outermost grinding ball

Figure 3.
Simulation of motion track of single grinding ball.

It can be seen from Figure 3 that the initial position at the edge of the ball mill is similar to the motion path of the ball in the middle. After 1-2 circles of operation in the ball mill, the liner plate will be stably lifted and then the throwing motion will be carried out. The ball in the middle dead zone will cycle around in a small range. If the ball mill is operated for a long time, the balls in the heavy middle dead zone will reach the edge of the ball mill from the middle dead zone due to the interaction, so as to be lifted for throwing motion. However, no matter the throwing movement or the creeping movement in the middle area, it can contact with the grinding particles to achieve the grinding effect.

3.2. Comparative Analysis of Ball Height

The liner plate of ball mill, especially the lifting strip, is mainly used to bring the ball to a certain height so that the ball can fall to a proper position to crush and grind materials with high efficiency [21]. Therefore, the ball height of the ball mill liner is one of the important indicators to evaluate the quality of the liner and the grinding efficiency. The impact of liner wear on the ball height can be analyzed through the average potential energy comparison of all the grinding ball media in the ball mill at the same time.

Edelweiss Applied Science and Technology
ISSN: 2576-8484
Vol. 9, No. 4: 651-662, 2025
DOI: 10.55214/25768484.v9i4.6037

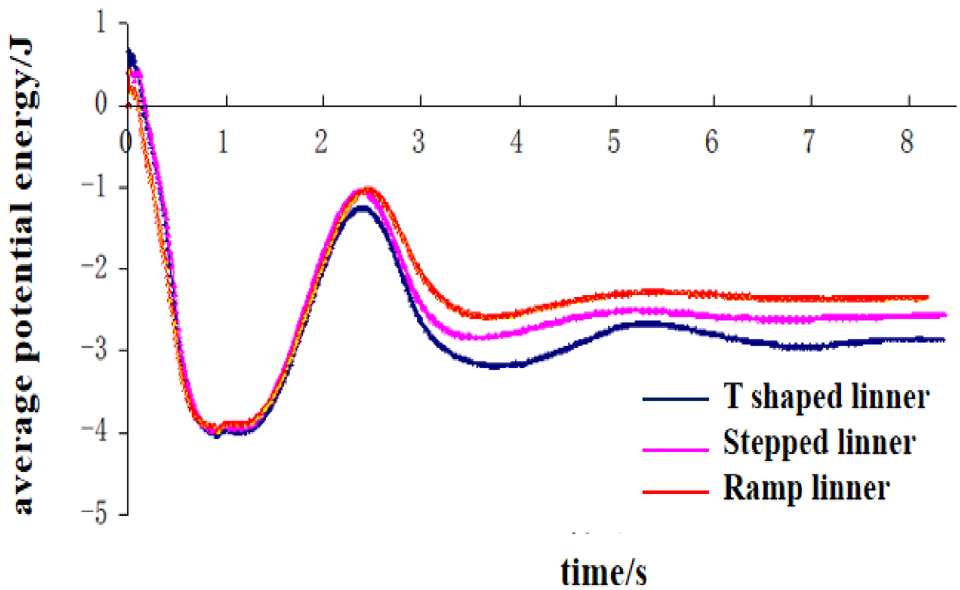

Figure 4.
Average potential energy—time curves of grinding ball at different liner plate structures.

Since the origin of the potential energy calculation is at the center of the ball mill cylinder, the average potential energy of the ball is negative. As shown in Fig. 4, when the ball reaches the equilibrium position (8s) of circulation, the average potential energy of the ball of the stepped liner plate is -2.57J, the average potential energy of the ball of the T shaped liner plate is -2.94J, and the average potential energy of the ball of the ramp liner plate is -2.34J. Since the T shaped liner strip has the most balls to throw down, the average potential energy of the balls is the largest, and theoretically it has the best effect on the lifting height of the balls. However, most of the balls in the throwing motion of the T-shaped liner do not fall into the accumulation area of the ore steel balls, but directly fall onto the liner plate. This part of the balls do not play an effective role in grinding, but cause loss to the liner plate of the ball mill.

Through the EDEM software post-processing tool, it can be observed that when the grinding process is in the balance position, the angle change of the internal ball inclined surface of the ball mill can judge the change of the effective ball height of the liner plate [22]. The smaller the angle of the inclined surface, the better the lifting effect.

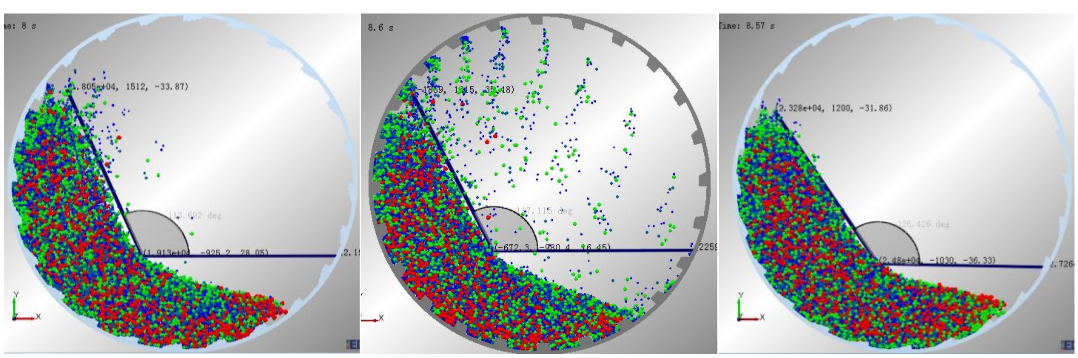

(a) Stepped liner plate (b) T shaped liner plate (c) Ramp liner plate

Figure 5.
Comparison of angle of inclined surface of grinding ball.

Edelweiss Applied Science and Technology
ISSN: 2576-8484
Vol. 9, No. 4: 651-662, 2025
DOI: 10.55214/25768484.v9i4.6037

Table 2.
Angle of inclined surface of grinding ball.

Type of liner plate	Stepped liner plate	T shaped liner plate	Ramp liner plate
Angle of inclined surface/℃	113.7	117.1	125.4

It can be seen from Figure 5 that the angle between the inclined surface of the grinding ball and the horizontal direction is 113.7° before the abrasion of the step-shaped liner plate, which is 3% and 9.3% higher than the T-shaped liner plate and the slope-shaped liner plate respectively. From this point of view, the effect of the step-shaped liner plate on the effective ball height is the best

3.3. Comparison And Analysis of Ball Mill Power

The power of ball mill is one of the most important indicators in the operation process of mill [23]. Under the same rotating speed and filling materials, the larger the power of ball mill is, the more the unit power consumption is, and the higher the production cost is Tohry, et al. [24]. In the ball mill EDEM simulation, the instantaneous torque Ti of the mill can be obtained, and then the average torque T of the mill can be calculated according to the instantaneous torque borne by the mill, and then the net driving power of the mill can be obtained from the average torque. The driving power here is called net driving power because other factors such as the transmission efficiency of the mill are not considered [25]. The driving power can be calculated by the following formula.

$$T = \frac{1}{n_i}\sum_{i=1}^{n_i} T_i \qquad (4)$$

$$P = \frac{2\pi n T}{60} \qquad (5)$$

Instantaneous torque within simulation time can be obtained through EDEM post-processing, as shown in Figure 6.

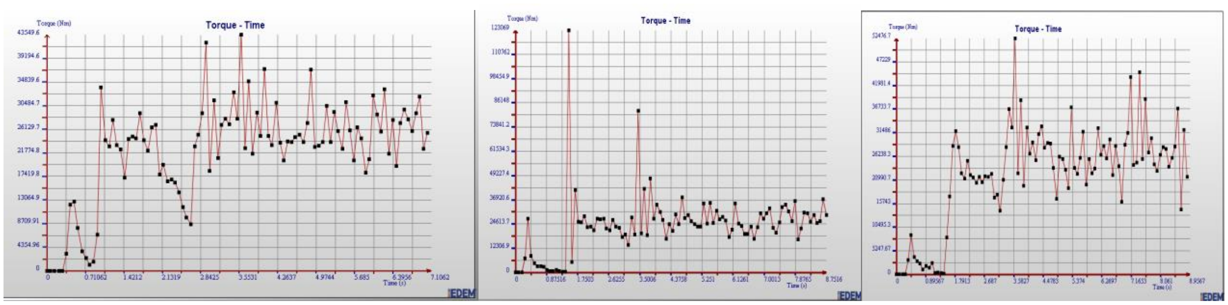

(a) Stepped liner plate (b) T shaped liner plate (c) Ramp liner plate

Figure 6.
Torque-time Curve of Ball Mill Barrel with Different Liner Structure.

It can be seen from Figure 6 that the torque fluctuation of the ball mill at the early stage of operation is large, indicating that the stability of the ball mill is poor at the beginning of operation and gradually becomes stable at the later stage. Calculate the average torque and driving power of ball mill according to formula (1) and (2), as shown in Table 3.

Table 3.
Calculated values of torque and power.

Type of liner plate	Stepped liner plate	T shaped liner plate	Ramp liner plate
Average torque/Nm	26914.5	28024.3	26431.7
Drive power/Kw	40.8	42.5	40.2

As shown in table 3, the maximum power of ball mill with T shaped liner plate is 42.5Kw. However, the power of ball mill with step liner plate changes little before and after wearing of liner plate.

Therefore, under the same working condition, the power consumption of ball mill with step liner plate can be reduced by 5% on average compared with T-shaped liner plate. This is consistent with the low operating current of 5070A ball mill compared with 5070B ball mill with T-shaped liner in actual operation.

3.4. Collision Type

The collision in ball mill can be divided into effective collision and invalid collision. The collision between materials and grinding balls and liners is effective collision [26]. The more the collision times are, the greater the material crushing probability is, the better the grinding effect is Geng, et al. [27] The useless collision is the collision between liner and grinding ball, which only increases the steel consumption. Since no material is added in the simulation, the collision between the grinding ball and the liner plate is determined as invalid collision, and the collision between the grinding ball and the ball is effective collision. By comparing the percentage of invalid collision in the total collision, the impact of liner plate structure on the collision type can be analyzed.

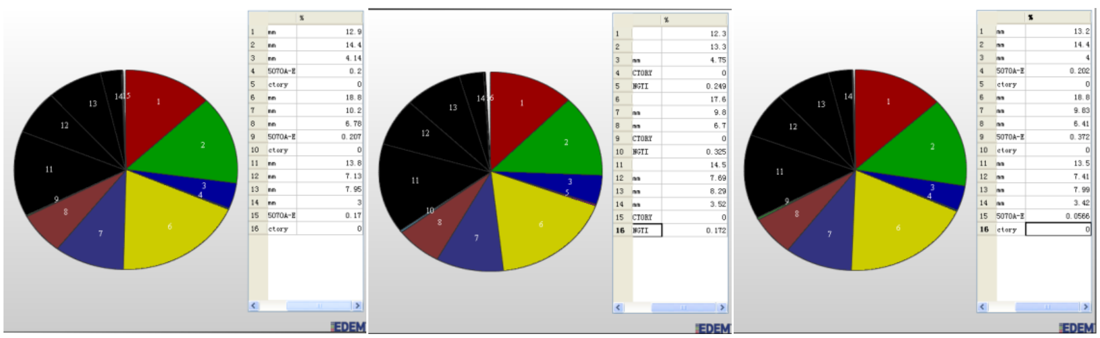

(a) Stepped liner plate (b) T shaped liner plate (c) Ramp liner plate

Figure 7.
Collision type comparison of ball mill.

Table 4.
Invalid collision ratio.

Type of liner plate	Stepped liner plate	T shaped liner plate	Ramp liner plate
Invalid collision ratio	0.90%	1.55%	1.04%

Based on the statistics of the proportion of invalid collision types in Figure 7 to the total collision, the data in Table 4 is obtained. The collision between the grinding ball and the lining plate of the stepped lining plate accounts for 0.90% of the total collision; The collision between the grinding ball of the T-shaped liner and the liner accounts for 1.55% of the total collision; In the worn stepped liner plate, the collision between the grinding ball and the liner plate accounts for 1.04% of the total collision. Therefore, under the same working condition, the T-shaped liner plate has the most invalid collision and the largest steel consumption, while the worn stepped liner plate has more collisions with the grinding ball than the liner plate before wearing, so the wearing speed of the liner plate will be faster and faster after wearing.

3.5. Collision Frequency and Relative Speed

The crushing energy of ore crushing is mainly affected by the motion state of the grinding ball medium, and the main factors determining the motion state of the grinding ball medium are: the structural parameters of the grinding chamber, the relative linear velocity of the grinding ball medium and the quality of the grinding medium. The relative velocity of the grinding ball directly determines the collision energy. When the collision energy is greater than the energy required for ore particle crushing, the ore will be crushed. Therefore, when the relative speed is greater than the critical speed of ore crushing, the more times the balls collide with each other, the better the grinding effect is.

$$E = \sum_i n_i \left(\frac{1}{2}mv_i^2 - \frac{1}{2}mv_a^2\right) \quad (6)$$

Where V_i is Relative velocity of ball medium, m/s; V_a is minimum relative velocity required for ore crushing, m/ ; n_i is number of particle collisions corresponding to the corresponding velocity.

The graph of relative speed and collision times can be obtained through simulation, and the collision times at a certain time point under relative speed can be obtained. It has been tested that ore can be crushed when the ball reaches a collision velocity of 1.7 m/s. In order to observe the number of collisions at high relative speeds, the abscissa relative speed is truncated and the number of collisions at relative collision speeds above 1.7 m/s (as shown in Figure 8) is observed and the data is summarized in Table 5.

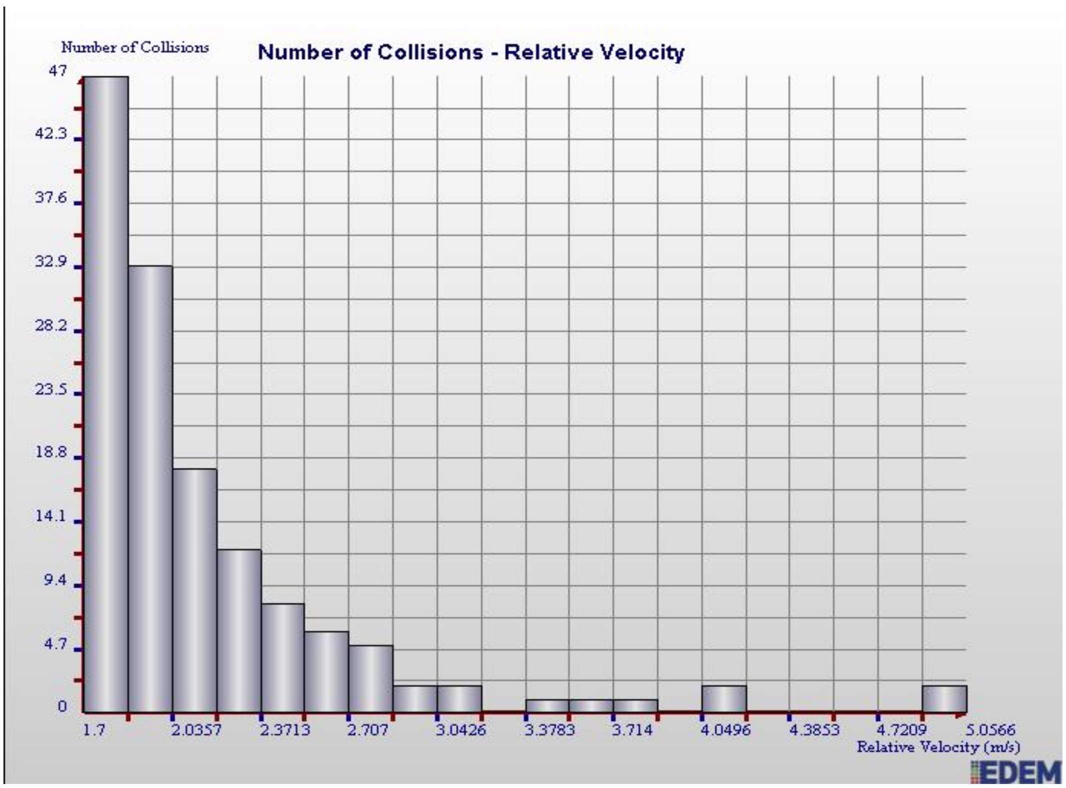

(a) Stepped liner plate

Edelweiss Applied Science and Technology
ISSN: 2576-8484
Vol. 9, No. 4: 651-662, 2025
DOI: 10.55214/25768484.v9i4.6037

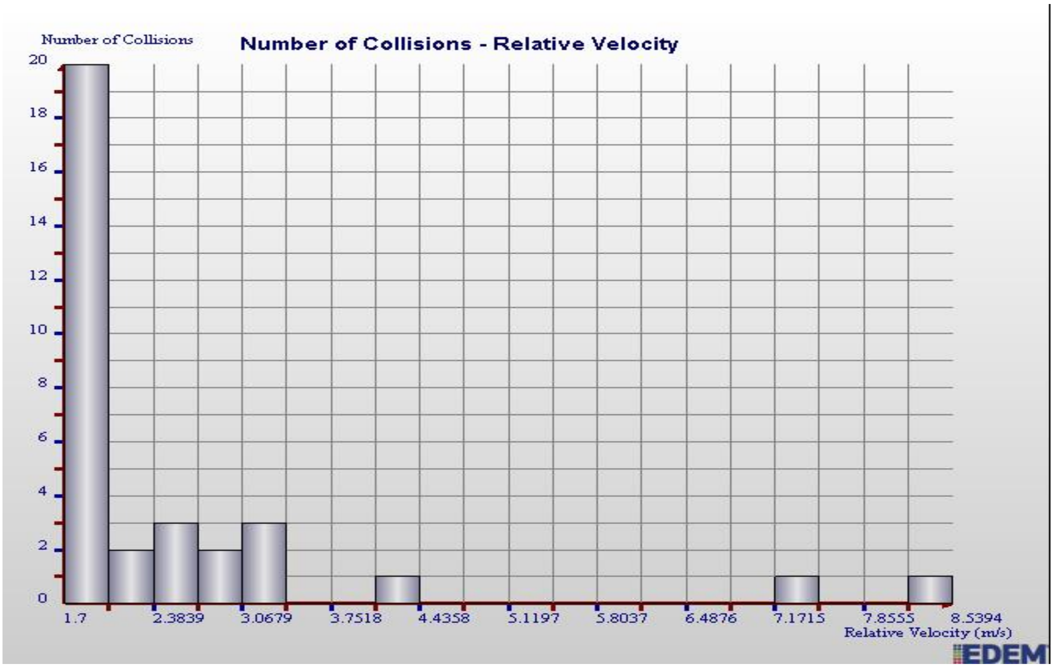

(b) T shaped liner plate

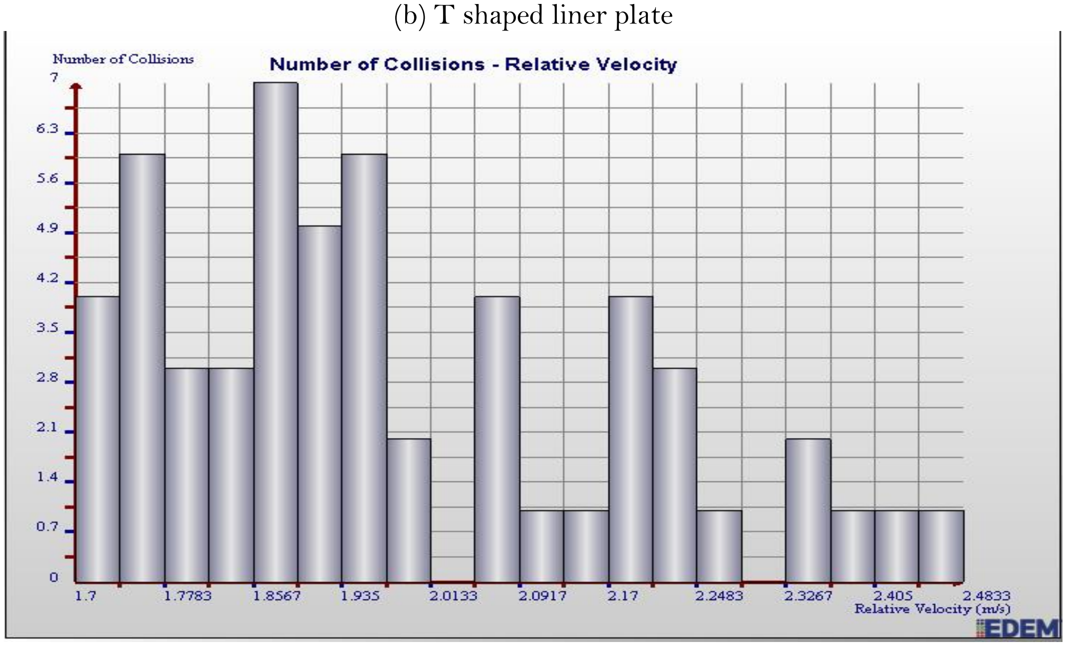

(c) Ramp liner plate

Figure 8.
"Number of collisions - relative velocity" for different structural liner.

Table 5.
Statistical Table of Ball Collision Times and Relative Velocity

Type of liner plate	Stepped liner plate	T shaped liner plate	Ramp liner plate
Total number of collisions	29365	14333	25117
Maximum relative velocity of collision /m/s	5.06	8.54	2.48
Collision times above 1.7m/s	144	33	53

Based on the simulation data statistics, when the mill is operating, the collision times within the relative speed of 1m/s account for more than 95% of the total collision times, indicating that the ball mill is mainly ground; It can be seen from Table 5 that the total number of ball collisions of the stepped liner is the largest, close to 30000, more than twice the number of collisions of the T-shaped liner. In terms of the maximum relative velocity of the ball, the maximum relative velocity of the T-shaped liner plate reaches 8.5 m/s, because part of the ball is thrown down. However, the maximum relative velocity during collision of ramp liner plate is the minimum, only 2.48m/s, and the grinding effect is the worst.

Intercept the relative velocity above 1.7m/s and the collision times, it can be found that although the maximum relative velocity of the T-shaped liner plate is the highest, the collision times are far less than that of the stepped liner plate; The ramp liner is significantly lower than the step liner in terms of both relative speed and number of collisions. It can be concluded that the stepped liner plate has a great advantage in terms of collision number and effective collision.

4. Conclusion

Through discrete element simulation of the grinding process of three different structured lining plates in a ball mill, analyze the motion trajectory and distribution state of the grinding balls. The comparative analysis of three different structures of lining plates was conducted using the evaluation indicators of increasing the height of grinding balls, collision speed, collision type, collision frequency, and relative speed. The results showed that compared with T-shaped lining plates and sloping lining plates, the effective ball height of stepped lining plates increased by 3% and 9.3% respectively, the ineffective collision ratio decreased by 0.65% and 0.15%, the power of T-shaped lining plates decreased by 5%, and the effective collision frequency was the highest. In summary, stepped lining plates have obvious advantages in grinding effect and energy consumption, which is consistent with the actual production results. This indicates that discrete element simulation can be effectively applied to simulate the grinding process of ball mills.

Transparency:

The authors confirm that the manuscript is an honest, accurate, and transparent account of the study; that no vital features of the study have been omitted; and that any discrepancies from the study as planned have been explained. This study followed all ethical practices during writing.

Acknowledgments:

Hunan Provincial Department of Education Science Research Project. China (21C1136).

References

[1] N. Matsanga, W. Nheta, and N. Chimwani, "A review of the grinding media in ball mills for mineral processing," *Minerals*, vol. 13, no. 11, p. 1373, 2023.

[2] P. Bortnowski, L. Gładysiewicz, R. Król, and M. Ozdoba, "Energy efficiency analysis of copper ore ball mill drive systems," *Energies*, vol. 14, no. 6, p. 1786, 2021.

[3] Z. Luo *et al.*, "Enhanced leaching of manganese from low-grade pyrolusite using ball milling and electric field," *Ecotoxicology and Environmental Safety*, vol. 211, p. 111893, 2021.

[4] A. Bor, B. Jargalsaikhan, K. Uranchimeg, J. Lee, and H. Choi, "Particle morphology control of metal powder with various experimental conditions using ball milling," *Powder technology*, vol. 394, pp. 181-190, 2021.

[5] W. Guo, Y. Han, Y. Li, and Z. Tang, "Impact of ball filling rate and stirrer tip speed on milling iron ore by wet stirred mill: analysis and prediction of the particle size distribution," *Powder Technology*, vol. 378, pp. 12-18, 2021.

[6] T. Wang, F. Zhang, J. Furtney, and B. Damjanac, "A review of methods, applications and limitations for incorporating fluid flow in the discrete element method," *Journal of Rock Mechanics and Geotechnical Engineering*, vol. 14, no. 3, pp. 1005-1024, 2022.

[7] Y. Guo and J. S. Curtis, "Discrete element method simulations for complex granular flows," *Annual Review of Fluid Mechanics*, vol. 47, no. 1, pp. 21-46, 2015.

[8] M. AmanNejad and K. Barani, "Effects of ball size distribution and mill speed and their interactions on ball milling using DEM," *Mineral Processing and Extractive Metallurgy Review*, vol. 42, no. 6, pp. 374-379, 2021.

[9] J. ZHANG *et al*., "Parameter Influence Analysis of Ball Mill Based on DEM," *UPB Scientific Bulletin Series D Mechanical Engineering*, vol. 85, no. 1, pp. 15-26, 2023.

[10] F. S. Mu, H. Li, X. X. Li, and H. Z. Xiong, "Jaw crusher based on discrete element method," *Applied Mechanics and Materials*, vol. 312, pp. 101-105, 2013.

[11] G. Cai, Y. Xiong, and L. Lin, "Experimental study on the fractal characteristics of rocks crushing," in *MATEC Web of Conferences*, 2015, vol. 25, p. 02008.

[12] K.-C. Kim, T. Jiang, N.-I. Kim, and C. Kwon, "Effects of ball-to-powder diameter ratio and powder particle shape on EDEM simulation in a planetary ball mill," *Journal of the Indian Chemical Society*, vol. 99, no. 1, p. 100300, 2022.

[13] H. Li, "Numerical simulation and analysis of vibration screening based on EDEM," vol. 27, no. 5, pp. 117-121, 2011.

[14] N. Stoimenov and J. Ruzic, "Analysis of the particle motion during mechanical alloying using EDEM software," *IFAC-PapersOnLine*, vol. 52, no. 25, pp. 462-466, 2019.

[15] M. Thomaz, "Newton's Second Law of a particle with variable mass," *Revista Brasileira de Ensino de Física*, vol. 43, p. e20210090, 2021.

[16] Y. Zhang and L. Li, "Introduction and implementation of fluid forces in a DEM code for simulating particle settlement in fluids," *Powder Technology*, vol. 433, p. 119238, 2024.

[17] C. Santos, V. Urdaneta, X. García, and E. Medina, "Compression and shear-wave velocities in discrete particle simulations of quartz granular packings: Improved Hertz-Mindlin contact model," *Geophysics*, vol. 76, no. 5, pp. E165-E174, 2011.

[18] S. Zhao, T. M. Evans, and X. Zhou, "Effects of curvature-related DEM contact model on the macro-and micro-mechanical behaviours of granular soils," *Géotechnique*, vol. 68, no. 12, pp. 1085-1098, 2018.

[19] M. Mhadhbi, "Effect of milling parameters on DEM modeling of a planetary ball mill," *Advances in Materials Physics and Chemistry*, vol. 13, no. 4, pp. 49-58, 2023.

[20] Z. Yin, Z. Jin, and T. Li, "Research on an Accurate Simulation Modeling and Charge Motion Quantitative Evaluation Method for Ball Mill in Confined Space," *Minerals*, vol. 14, no. 6, p. 604, 2024.

[21] J. Gawlik, J. Schmidt, T. Nowak, Z. Wójcicki, and A. Zagórski, "Nitrogen as an alloying element improving material properties of the high carbon cast steel for ball mill liner plates," *Archives of Civil and Mechanical Engineering*, vol. 17, no. 4, pp. 926-934, 2017.

[22] Z. Li, Y. Wang, K. Li, W. Lin, and X. Tong, "Study on the Performance of Ball Mill with Liner Structure based on DEM," *Journal of Engineering & Technological Sciences*, vol. 50, no. 2, 2018.

[23] V. Gupta and S. Sharma, "Analysis of ball mill grinding operation using mill power specific kinetic parameters," *Advanced Powder Technology*, vol. 25, no. 2, pp. 625-634, 2014.

[24] A. Tohry, S. C. Chelgani, S. Matin, and M. Noormohammadi, "Power-draw prediction by random forest based on operating parameters for an industrial ball mill," *Advanced Powder Technology*, vol. 31, no. 3, pp. 967-972, 2020.

[25] X. Bian, G. Wang, H. Wang, S. Wang, and W. Lv, "Effect of lifters and mill speed on particle behaviour, torque, and power consumption of a tumbling ball mill: Experimental study and DEM simulation," *Minerals Engineering*, vol. 105, pp. 22-35, 2017.

[26] L. M. Tavares, "A review of advanced ball mill modelling," *KONA Powder and Particle Journal*, vol. 34, pp. 106-124, 2017.

[27] F. Geng, L. Gang, Y. Wang, Y. Li, and Z. Yuan, "Numerical investigation on particle mixing in a ball mill," *Powder Technology*, vol. 292, pp. 64-73, 2016.